*Desalination and Water Treatment*
www.deswater.com

doi: 10.1080/19443994.2013.811112

52 (2014) 5681–5695
August

Taylor & Francis
Taylor & Francis Group

# Removal of Ni(II) from aqueous system by chemically modified sunflower biomass

Monika Jain[a], Vinod Kumar Garg[a,*], Krishna Kadirvelu[b]

[a]*Department of Environmental Science and Engineering, Guru Jambheshwar University of Science and Technology, Hisar 125001, Haryana, India*
*Tel. +91 1662 275375; Fax: +91 1662 276240; email: vinodkgarg@yahoo.com*
[b]*Defence, Bioengineering & Electromedical Laboratory (DEBEL), Defence Research & Development Organization, Raman Nagar, Bangalore 560093, India*

Received 23 January 2013; Accepted 11 May 2013

ABSTRACT

This study reports the removal of Ni(II) onto boiled sunflower head (BSH) and formaldehyde sunflower head (FSH) adsorbents by batch technique. The adsorbents were characterized by Fourier transform infrared spectrometer (FTIR), scanning electron microscopy (SEM), and energy dispersive X-ray (EDX) analysis. The results showed that Ni(II) adsorption was dependent on process operating conditions including pH of the solution, adsorbent dosage, temperature, and initial Ni(II) ion concentration in the solution. The optimum pH for Ni(II) was 6.0. Maximum nickel adsorption was 65.5 and 75.9%, respectively, by BSH and FSH at adsorbent dose = 20.0 g/L, initial Ni(II) concentration = 100 mg/L, temperature = 25 ± 1˚C. Langmuir and Freundlich isotherm models were used to analyze the equilibrium adsorption data. Freundlich isotherm fitted the data well with $R^2$ values >0.99 for both the adsorbents. The results also showed that pseudo-second-order kinetic model correlated well with the adsorption data with $R^2$ values >0.99 for both the adsorbents.

*Keywords:* Adsorption; Heavy metals; Adsorbent; FTIR; Desorption

## 1. Introduction

Environmental pollution by heavy metals is a serious issue due to their toxicity and nonbiodegradable nature. Nickel in trace amounts may be beneficial as an activator of some enzyme systems but also known for its neurotoxicity and carcinogenicity [1]. Though nickel is an essential micronutrient for animals and takes part in synthesis of Vitamin $B_{12}$ [2], its higher concentration causes cancer of lungs, nose, and bone [3]. Ni(II) contamination in drinking water may cause severe damage to lungs, kidneys, gastrointestinal distress, for example, nausea, vomiting, diarrhea, pulmonary fibrosis, renal edema, and skin dermatitis [3].

Nickel is released from various industries like nickel plating, silver refinery, zinc-based casting industry and storage batteries, mining and metallurgy of nickel, stainless steel, ceramic industry, paint formulation, porcelain enameling etc. Conventional methods for nickel removal from water and wastewater include ion exchange, chemical precipitation, coagulation–flocculation, complexation, chemical reduction, solvent extraction etc. But these methods involve high capital cost with recurring expenses that

---

*Corresponding author.

are not suitable for small-scale industries. Adsorption is considered to be an effective purification and separation technology for wastewater treatment. It is a clean technology which removes heavy metals even at very low concentration (less than 100 mg/L). Adsorption technology employing industrial wastes, microorganisms, and agricultural wastes (plant wastes) has been employed by many researchers in last few decades.

Plant biomass has emerged as an attractive option to develop adsorbents due to their nontoxic, selective, efficient and inexpensive and easy regeneration properties. The sorption of heavy metals by these kind of materials might be attributed to their proteins, carbohydrate and phenoloic compounds. These compounds contain biopolymers like carboxyl, carbonyl, hydroxyl, amino group, amine, imine, alcohols, ketones that can bind metal ions and are supposed to be the active sites for the sorption of metal ions [4]. Several researchers have advocated the chemical modification or pretreatment of these materials to enhance their efficiency [5].

The adsorbents have been chemically modified using different kinds of modifying agents like base solutions (sodium hydroxide, sodium carbonate, calcium hydroxide), mineral and organic acid solutions (hydrochloric acid, sulfuric acid, nitric acid, and citric acid), organic compounds (ethylenediamine, formaldehyde, and methanol), oxidizing agents (hydrogen peroxide) for the purpose of removing soluble organic compounds, eliminating color of aqueous solution and increasing efficiency of metal adsorption [6]. Salem and Awad [7] modified loquat bark waste (*Eriobotrya japonica*) with 0.1 N sodium hydroxide. The Ni(II) adsorption was achieved upto 91.8% from electroplating wastewater using this material. Krishnan et al. [1] reported that adsorption capacity of sugarcane bagasse pith–based activated carbon was 140.85 mg/g, while it was 73.56 mg/g for raw sugarcane bagasse pith.

Sunflower (*Helianthus annuus)* is an oil seed crop. The plant was chosen as the raw material for the preparation of adsorbent because of its relative abundance in Haryana and lack of information about its sorption capacity toward the adsorption of Ni(II). The residual material from sunflower head after threshing out seed is a waste material and not put to any use. A bibliographic survey has shown that only a few studies have been carried out on sunflower stem biomass for heavy metal removal from the water but no information is available on Ni(II) removal from aqueous solution by dried sunflower head biomass. Sun and Xu [8] studied adsorption potential of sunflower stalks for the removal of dyes. They found that maximum adsorption capacity was 205 and 317 mg/g for methylene blue and basic red 9, respectively. In another study, Sun and Shi [9] studied the removal of copper, cadmium, zinc, and chromium from aqueous solution using sunflower stalks. The maximum adsorption of four heavy metals was 29.3 mg/g ($Cu^{2+}$), 30.73 mg/g ($Zn^{2+}$), 42.18 mg/g ($Cd^{2+}$), and 25.07 mg/g ($Cr^{3+}$), respectively. Thinakaran et al. [10] prepared the activated carbon using sunflower seed hull and studied its dye removal potential. The adsorption capacity

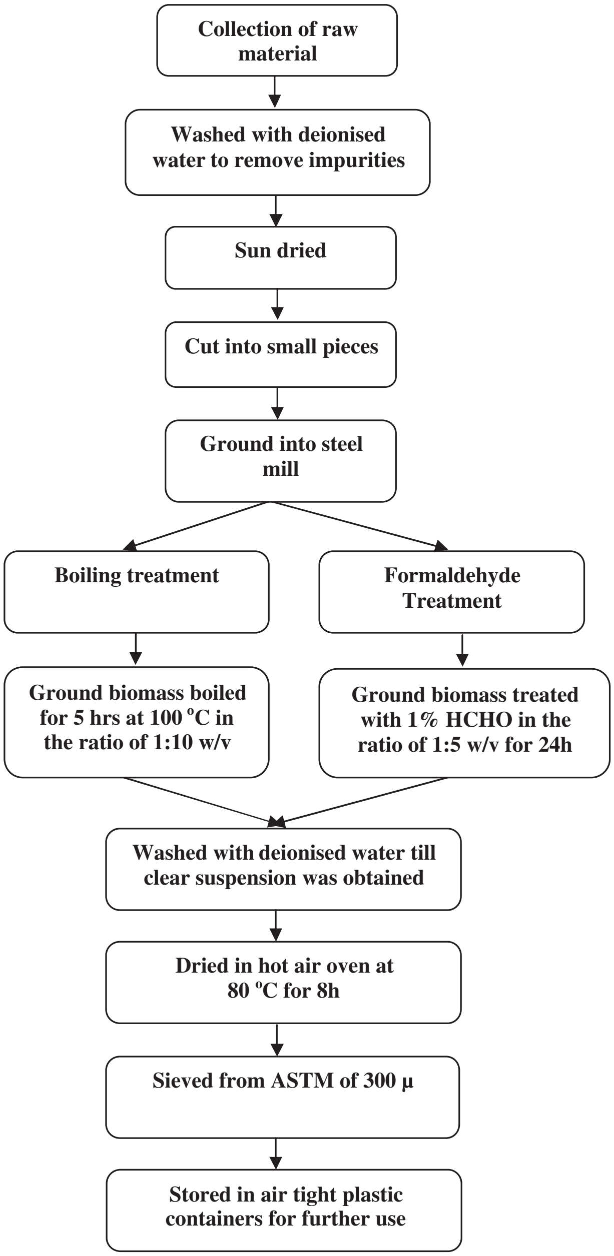

Fig. 1. Schematic diagram of adsorbent preparation.

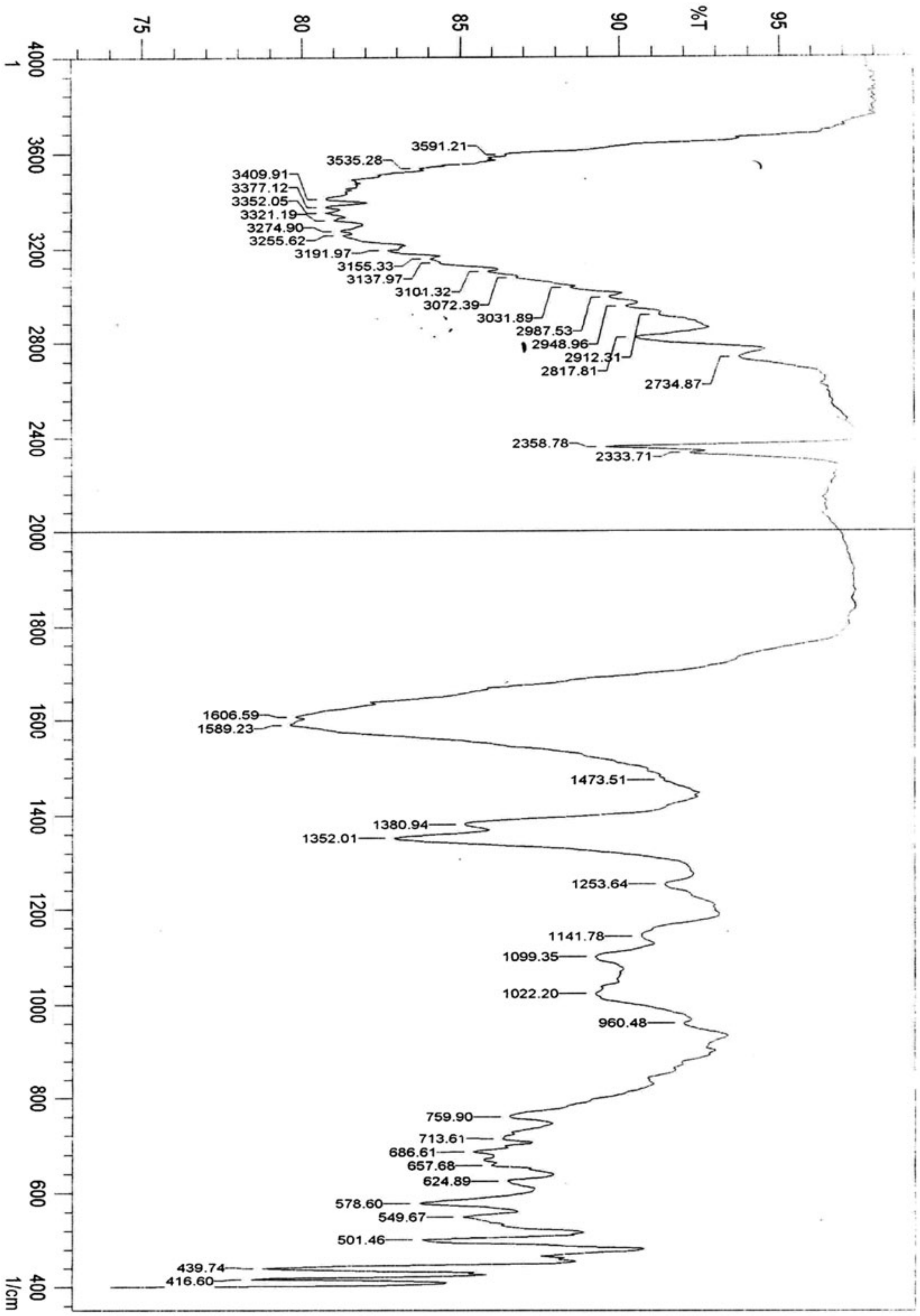

Fig. 2A. FTIR spectrum of native BSH adsorbent.

was found to be approximately 65%. So, in the present study, an effort has been made to chemically modify sunflower head waste with formaldehyde and compare its adsorption capacity with raw material.

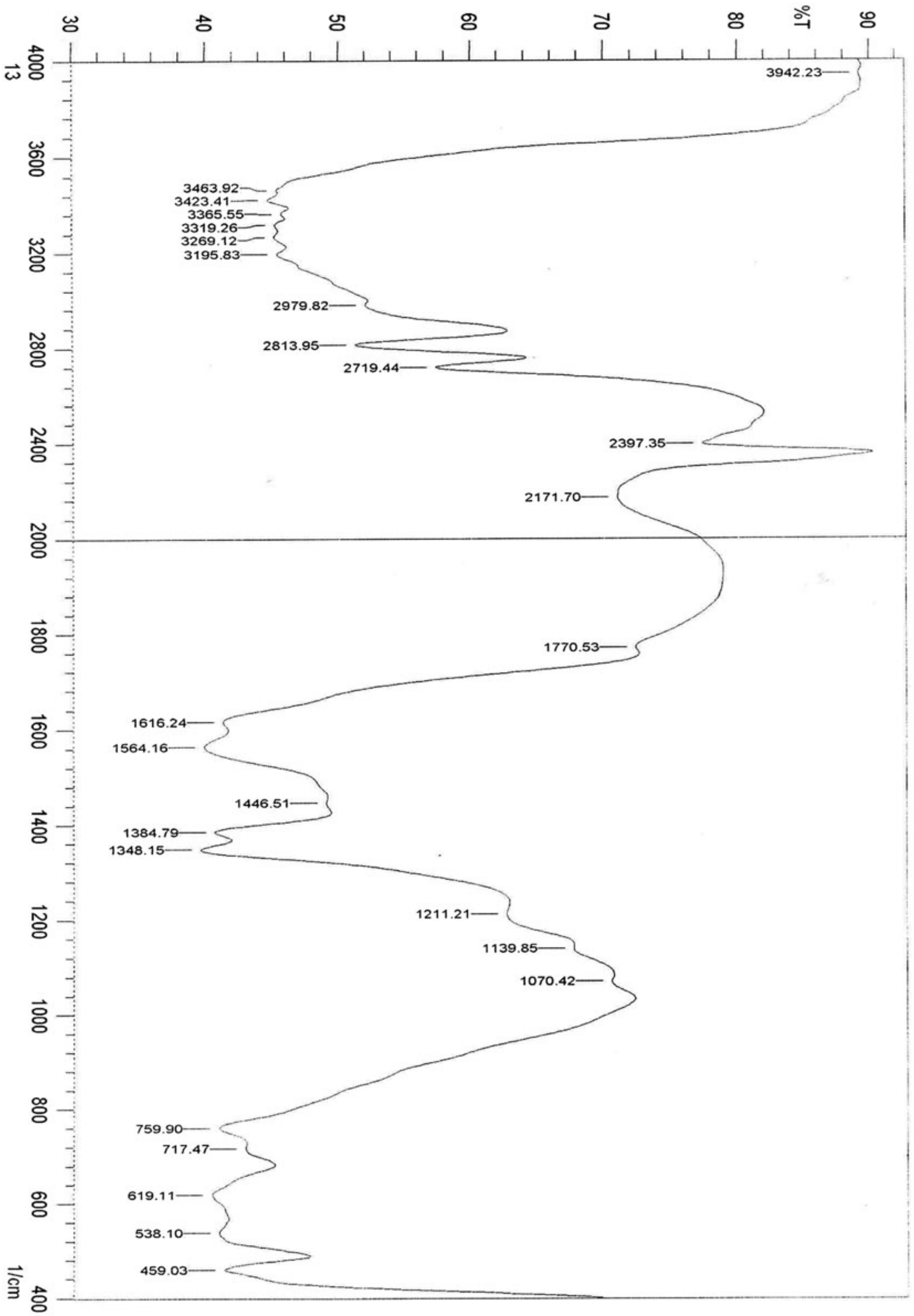

Fig. 2B. FTIR spectrum of Ni(II)-loaded BSH adsorbent.

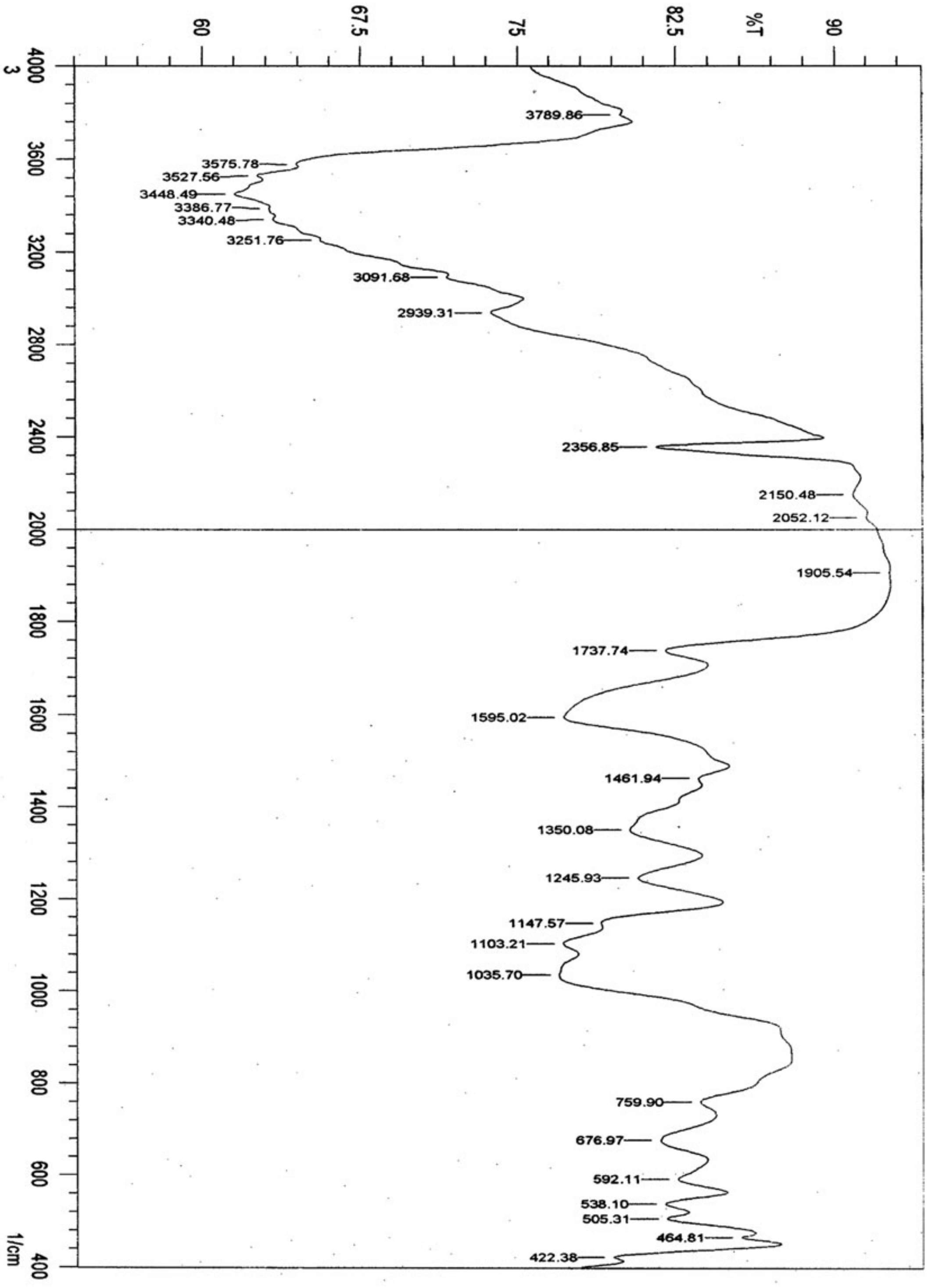

Fig. 2C. FTIR spectrum of native FSH adsorbent.

## 2. Materials and methods

### 2.1. Preparation of adsorbents and their characterization

Two adsorbents viz., boiled sunflower head (BSH) and formaldehyde treated sunflower head (FSH) were prepared from deseeded heads of *Helianthus annuus* plant (Fig. 1) as reported by Jain et al. [11]. The purpose of using formaldehyde for pretreatment of biomass was to mask the color of the biomass so that it does not leach out into the aqueous solution.

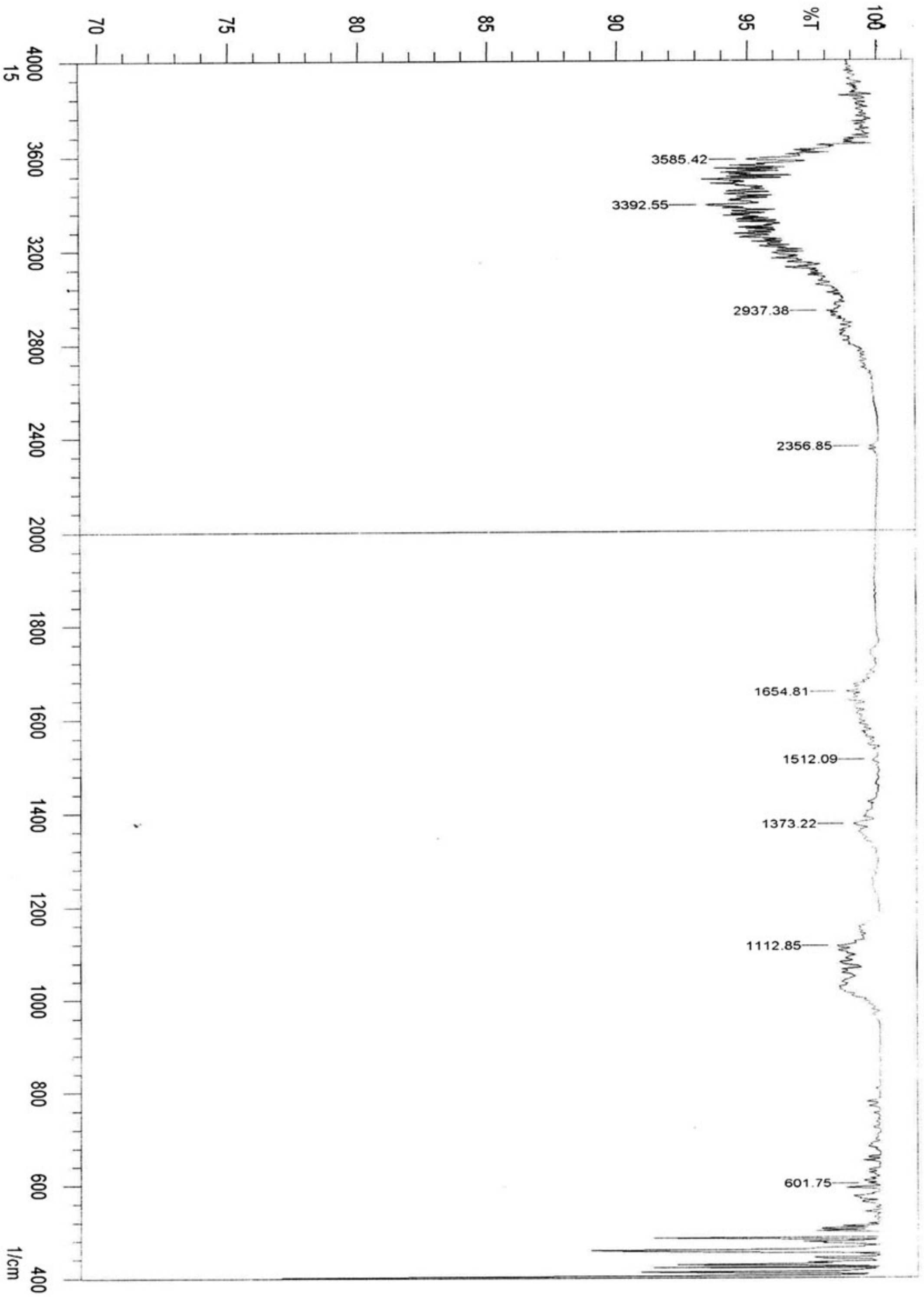

Fig. 2D. FTIR spectrum of Ni(II)-loaded FSH adsorbent.

FTIR spectra of native and Ni(II)-loaded adsorbents were recorded in the range of 400–4,000 $\text{cm}^{-1}$ to obtain the information about the functional groups present on the adsorbents using Fourier transform infrared spectrometer (FTIR-8400S, Shimadzu, Japan). The surface morphology and elemental deposition on

Table 1
Fundamental FTIR frequencies of native and Ni(II)-loaded adsorbents

| Biosorbents (native and metal loaded) | Fundamental frequencies ($cm^{-1}$) | | | | |
|---|---|---|---|---|---|
| | –OH/–N–H | –C–H | –C=O | $–OCH_3$/–C–N | Bending vibrations |
| BSH (native) | 3535.28–3155.33 | 2817.81 | 1606.59 | 1141.78, 1099.35 | 759.90, 578.60, 439.74 |
| BSH–Ni(II) loaded | 3463.92–3195.83 | 2813.95 | 1616.24 | 1139.85, 1070.42 | 759.90, 538.1, 459.03 |
| FSH (native) | 3575.78–3251.76 | 2939.31 | 1737.74 | 1147.57, 1035.70 | 759.90, 676.97, 592.11 |
| FSH–Ni(II) loaded | 3585.42–3392.95 | 2937.38 | 1654.81 | 1112.85 | 601.75 |

the surface of the adsorbents was visualized via Scanning electron microscopy (SEM) and energy dispersive X-ray analysis (EDX) (model Quanta 200 FEG, FEI, the Netherlands). The elemental composition of the adsorbents was determined using elemental analyzer. Surface area analysis of the adsorbents was carried

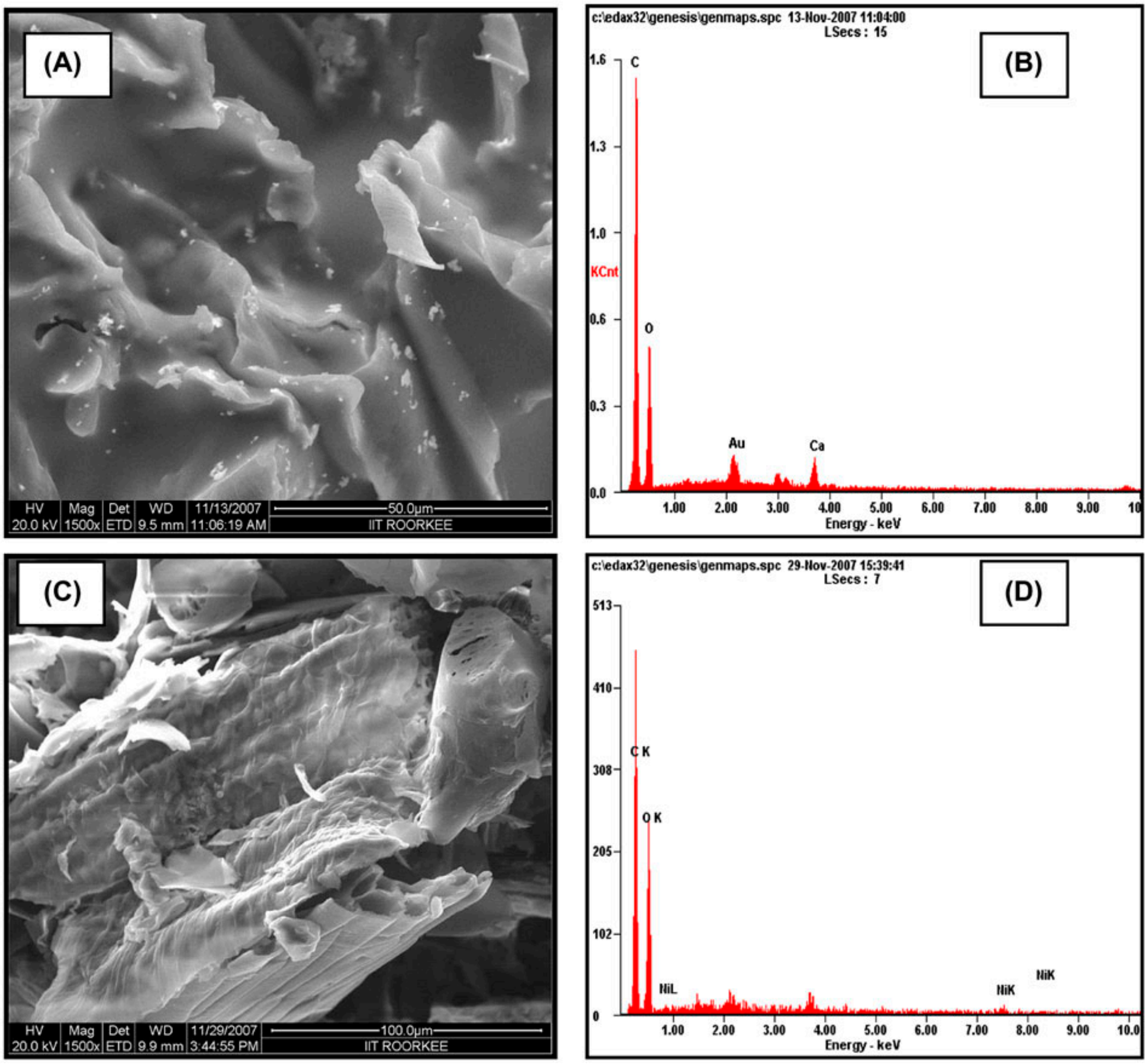

Fig. 3. (A) SEM of native BSH, (B) EDX of native BSH, (C) SEM of Ni(II)-loaded BSH, (D) EDX of Ni(II)-loaded BSH (E) SEM of native FSH, (F) EDX of native FSH, (G) SEM of Ni(II)-loaded FSH, and (H) EDX of Ni(II)-loaded FSH.

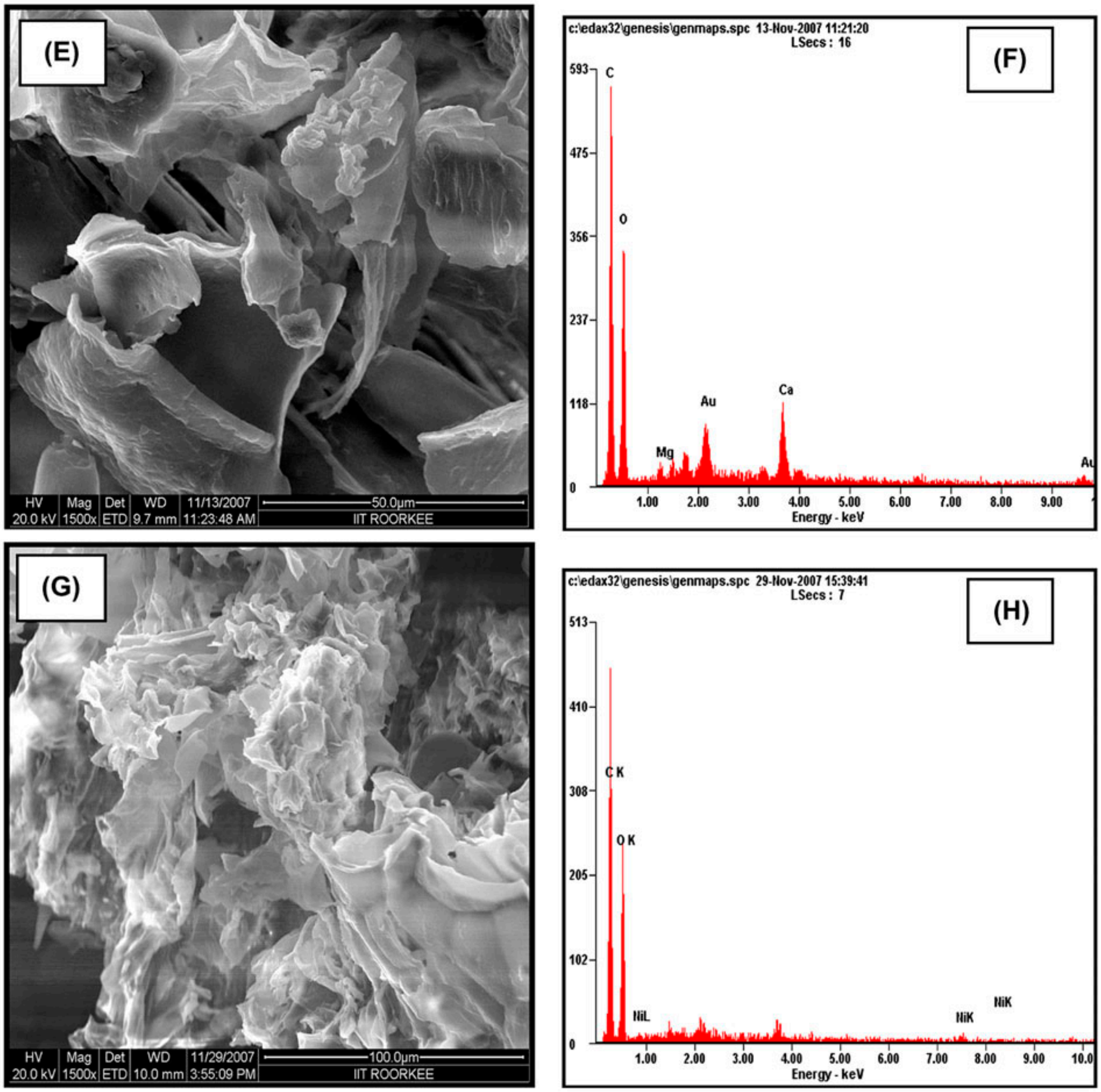

Fig. 3. (*Continued*)

out using surface area analyzer (Micromeritics, Japan, model no. ASAP-2010).

### 2.2. *Adsorption studies*

Stock solution of Ni(II) of 1,000 mg/L concentration was prepared using $Ni(NO_3)_2.6H_2O$ in double-distilled water acidified with nitric acid to prevent hydrolysis. The stock solution was further diluted with distilled water to obtain required standard solution. The pH of the solution was adjusted to required value by adding either 0.01 M HCl or 0.01 M NaOH using pH meter calibrated with buffers of pH 4.0, 7.0, and 9.2. The equilibrium concentration of metal ions in the aqueous solution was measured using Atomic Absorption Spectrophotometer (Shimadzu 6300, Japan). The instrument was calibrated within linear range of analysis, and a correlation coefficient of 0.98 or greater was obtained for calibration curve.

Equilibrium adsorption experiments were carried out in 150-mL Erlenmeyer flasks at optimized pH of 6.0 by adding 1.0 g of sorbent to 50 mL of Ni(II) solution at 25 ± 1 °C temperature. The adsorbents were separated from the solution after 3.0 h by centrifugation at 4,000 rpm. The residual metal ion concentration in the supernatant was estimated as reported earlier using AAS. Blank samples were also run under similar experimental conditions without adsorbent to correct for any adsorption on the internal surface of flasks.

The percent nickel removal ($R\%$) was calculated for each run using Eq. (1):

$$R(\%) = \frac{C_i - C_e}{C_i} \times 100 \tag{1}$$

where $C_i$ and $C_e$ were the initial and equilibrium Ni (II) concentrations in the solution in mg/L. The unit adsorption $q_e$ (mg of metal per g of adsorbent) was determined using Eq. (2):

$$q_e\ (\text{mg/g}) = \left[\frac{C_i - C_e}{M}\right] \times V \tag{2}$$

where $C_i$ and $C_e$ are same as above, $V$ is the volume of the solution in (L), and $M$ is the mass of the biosorbent (g).

## 3. Results and discussion

### 3.1. Adsorbent characterization

The adsorbents were characterized by surface area analysis, FTIR, SEM, EDX, and elemental composition. The surface area of an adsorbent depends on its structure; the more pores and greater surface area it has which has a significant influence on its adsorption capacity. In this study, the adsorbents were sieved to get the particle size of $\leqslant 300\ \mu$ in order to increase the total surface area and provide more sorption sites for adsorption. Surface area of BSH and FSH was 1.72 and 1.91 $m^2/g$, respectively.

The FTIR spectra of native and Ni(II)-loaded adsorbents are given in Fig. 1. The FTIR spectra of native BSH adsorbent (Fig. 2A) has intense peaks at 2,700–3,500 $cm^{-1}$ representing –OH group stretching, stretching of carboxylic group and –NH groups showing the presence of hydroxyl and amine groups indicated by the broad peaks at 3409.91 and 3155.33 $cm^{-1}$. The peak around 2817.81 $cm^{-1}$ indicates the existence of $-CH_2$ asymmetric stretching vibrations due to methylene group (Table 1). The peaks at 1606.59 $cm^{-1}$ corresponds to carbonyl groups of –C=O and –C–OH stretching from aldehyde and ketones. The bands appearing at 1589.23 and 1380.94 $cm^{-1}$ may be due to formation of oxygen functional groups like a highly conjugated –C=O stretching in carboxylic group and carboxylate moieties. The peak at 1141.59 $cm^{-1}$ is assigned to alcoholic –C–O and –C–N stretching vibration showing the presence of hydroxyl and amine group. The peak at 1099.35 $cm^{-1}$ may be attributed to –C–N stretching while the peak at 1022.20 $cm^{-1}$ indicated stretching of many –C–OH and –C–O–C bonds. The peaks corresponding to 1141.78, 1099.35, 1022.20 $cm^{-1}$ (sugar region = 790–1,180 $cm^{-1}$), 1473.51, 1589.23, 1606.59 $cm^{-1}$ (protein region = 1,400–1,700 $cm^{-1}$), 1253.64 $cm^{-1}$ (nucleic acid region) are present in the spectra of native BSH [12].

The FTIR spectra of Ni(II)-loaded BSH adsorbent (Fig. 2B) have broad peaks at 3463.92–3195.83 $cm^{-1}$ showing the presence of hydroxyl and amine groups (Table 1). The band at 3409.91 $cm^{-1}$ shifted to 3463.92 $cm^{-1}$ showing that the hydroxyl group was involved in Ni(II) binding. The peak at 1606.59 $cm^{-1}$ shifted to 1616.24 $cm^{-1}$ indicating the involvement of –C=O group in Ni(II) binding. The band at 1589.23 and 1380.94 $cm^{-1}$ shifted to 1512.09 and 1373.22 cm, respectively. The peaks at 1141.78 and 1099.35 $cm^{-1}$ shifted to 1139.85 and 1070.42 $cm^{-1}$, respectively. Shifting of the peaks in Ni(II)-loaded adsorbent indicates the involvement of the corresponding functional groups in Ni(II) adsorption.

In the native FSH adsorbent (Fig. 2C), the absorption peak at 3448.49 $cm^{-1}$ is due to –O–H stretching. Absorption peak at 2939.31 $cm^{-1}$ is indicative of the existence of $-CH_2$ asymmetric stretching vibration and symmetric –C–H stretching of aliphatic group (Table 1). The absorption peak at 2356.85 $cm^{-1}$ is assigned to P–H group. The distinct absorption peak at 1737.74 $cm^{-1}$ may be assigned to –C=O stretching band from the protonated carboxylic groups or ester groups. The absorption peak at 1147.57 $cm^{-1}$ may be due to –C–O stretching of ester group and the peak at 1035.70 is due to –C–O–C– group. The intensity of peaks was either minimized or shifted in case of Ni (II)-loaded FSH adsorbent (Fig. 2D). The peak at 3448.49 $cm^{-1}$ shifted to 3445.62 $cm^{-1}$ after nickel adsorption (Table 1). The shifting of this band indicates the involvement of N–H and O–H group in the adsorption process. The shift of carboxyl-stretching band to lower frequency (1730.12 $cm^{-1}$ from 1737.74 $cm^{-1}$) is also visible in the spectra. The peak at 1147.57 and 1035.70 shifted to 1112.85 and 1030.22 in Ni(II)-loaded FSH.

The SEM micrographs of native and Ni(II)-loaded BSH and FSH were recorded at 1500× magnification. SEM showed changes in surface morphology of the adsorbents before and after adsorption of nickel ions (Fig. 3). The SEMs of native adsorbent have rough, multilayered, and amorphous structure with no definable surface, while the surface of the biosorbents become smooth after Ni(II) adsorption. The EDX images of native adsorbents shows the presence of $Ca^{2+}$ and $Mg^{2+}$ peaks, while the EDX images of Ni(II) loaded adsorbents shows disappearance of $Ca^{2+}$ and $Mg^{2+}$ peaks and appearance of $Ni^{2+}$ peaks (Fig. 3A–H). Hence, the removal of Ni(II) ions may be an ion-exchange mechanism as well as adsorption [13]. The appearance of gold in the spectra is due to the fact that the adsorbent samples were coated with gold prior to analysis. EDX analysis therefore provided direct evidence for the specific adsorption of Ni (II) ions onto the adsorbents. Various elemental atoms are present in adsorbent (C, H, N, S, and O). These have their origin in the raw material and introduced during preparation or treatments [14]. These atoms significantly influence the charge, electronic density, and nature of the adsorbents. The percentage of C, H, N, and O in BSH was 39.3, 5.3, 0.84, and 54.5, respectively while in FSH, it was 39, 5.3, 0.85, and 54.8, respectively. The results show that sulfur was absent in both the adsorbents and the percentage of C, H, N, and O was almost equal in both the adsorbents.

### 3.2. *Effect of pH on nickel(II) adsorption*

Ni(II) adsorption experiments were carried out in the pH range of 2.0–6.0 at constant initial Ni(II) concentration (100 mg/L), adsorbent dose (20.0 g/L), stirring speed (180 rpm), and temperature (25 ± 1 °C) for 180 min. The effect of pH on Ni(II) adsorption is given in Fig. 4 A control for Ni(II) removal without adsorbent was also studied (Fig. 3). The results of control experiment revealed that there was no effect of pH on Ni(II) concentration in the solution upto pH 6.0. But when the pH was >6.0, Ni(II) concentration in solution decreased significantly. This may be due to precipitation of Ni(II) as Nickel hydroxide [$(Ni(OH)_2$] and $[NiOH]^+$ [15]. Keeping this in view, the adsorption studies were undertaken in the pH range of 2.0–6.0.

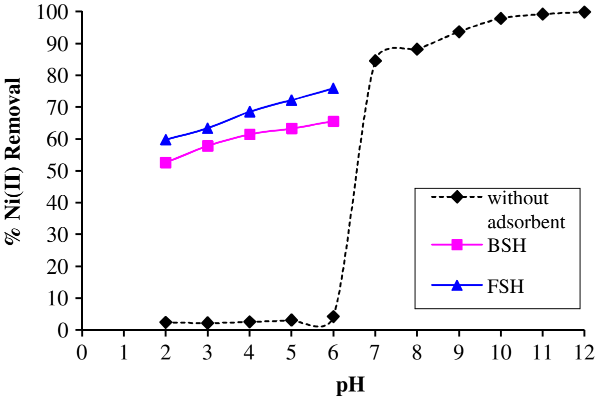

Fig. 4. Effect of pH on Ni(II) removal by BSH and FSH at initial Ni(II) conc. = 100 mg/L, adsorbent dose = 20.0 g/L, contact time = 3.0 h, temp. = 25 ± 1 °C, stirring speed = 180 rpm.

The results showed that, maximum Ni(II) adsorption was 65.5 and 75.9% by BSH and FSH (Fig. 4) at pH 6.0. So, pH 6.0 was selected as the optimum pH for further experiments. The adsorption capacity for Ni(II) increased from 2.6 to 3.3 mg/g by BSH and 2.9 to 3.8 mg/g by FSH as pH was enhanced from 2.0–6.0.

The adsorption of metal ions depends upon the nature of adsorbent surface and species distribution of metal ions in aqueous solution. Nickel(II) removal by BSH and FSH increased with increase in pH from 2 to 10. In the pH range of 7–12, maximum adsorption was observed. This might be due to hydrolysis of metal ion resulting in the formation of $NiOH^+$ and $Ni(OH)_2$. In the acidic pH range, nickel is present predominantly as $Ni^{2+}$ for adsorption leading to low removal of nickel ions. The experimental results of the effect of pH on nickel removal show an adsorption mechanism by ion exchange which is further confirmed by desorption [36,37]. It has further been explained by Brasquet et al. in the speciation diagram that $Ni^{2+}$ exist at pH=2, $NiO_2$ at pH=9, $NiOH^+$ and $Ni(OH)_2$ at pH=10 and $Ni(OH)_4$ and $Ni(OH_3)^-$ at pH=12 [38].

Under acidic solution conditions, both the adsorbents and the metal ions are positively charged ($M^{2+}$ and $H^+$) due to the formation of hydronium ions ($H_3O^+$) which leads to an electrostatic repulsion between the two [16]. Moreover, higher concentration of hydrogen ions in the aqueous medium competes with positively charged metal ions for surface adsorption, thereby leading to a decrease in the removal of Ni(II) at lower pH. But when the pH is increased, the $H^+$ ion concentration decreases and $OH^-$ concentration increases leading to electrostatic attraction between positively charged metal ions and negatively charged adsorbent surface resulting in an increase in metal removal. Friis and Myers-Keith [17] have reported that metal adsorption occurs due to ionization of negative functional molecular groups present on the adsorbent surface which serve as the binding sites. With the increase in pH, the degree of ionization of negative groups present on the adsorbent increases and the competing effect of $H_3O^+$ ions decreases, thus, increasing the adsorption of Ni(II) ions on the free binding sites.

### 3.3. *Effect of adsorbent dose*

Effect of adsorbent dose on Ni(II) adsorption was studied at constant initial Ni(II) concentration (100 mg/L), temperature (25 ± 1 °C), contact time (3 h), and stirring speed (180 rpm) by varying the adsorbent dose from 0.2 to 1.2 g/50 mL. The results are given in Fig. 5. The results indicate that percent Ni(II) adsorption increased with increase in adsorbent dose. This might be due to the availability of more surface functional groups on the surface of the adsorbent and higher surface area available for adsorption of Ni(II) ions [18]. Very slow increase in removal beyond an optimum dose may be attributed to the attainment of equilibrium between metal ions and adsorbent at the existing operating conditions. Unit adsorption decreased from 12.42–3.28 mg/g and 14.18–3.8 mg/g for BSH and FSH, respectively. This may be due to overlapping and aggregation of adsorbent particles on the adsorption sites which leads to a decrease in adsorption capacity at higher dose [19]. Similarly, Shukla et al. [20] have reported that the increase in percent adsorption with the increase in adsorbent dose may be due to the fact that when sorbent ratio is small, the active sites for binding metal ions on the adsorbent surface are also lesser, so the percent adsorption is low. When adsorbent dose is increased, more metal ions are adsorbed. Thus, it results in an increment of percent adsorption until saturation.

### 3.4. Effect of initial Nickel(II) ion concentration

The effect of initial metal ion concentration on Ni(II) removal by BSH and FSH is given in Fig. 6. The study was carried out at pH 6.0, contact time (3 h) and adsorbent dose (20 g/L), temperature (25 ± 1 ℃) and agitation speed (180 rpm). The data showed that Ni(II) removal decreased with increase in metal ion concentration. The Ni(II) removal decreased from 78.8–56.7% by BSH and 86.5–67.8% by FSH. This decrease in percent removal may be due to nonavailability of surface area to accommodate more Ni(II) ions. At lower concentration, all Ni(II) ions present in the solution interact with binding sites and thus removal is higher, whereas at higher concentration, percent removal is lower due to saturation of all the binding sites present on the surface of the adsorbent.

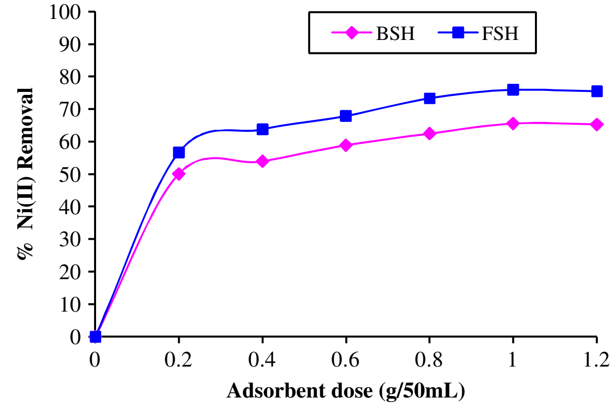

Fig. 5. Effect of adsorbent dose on Ni(II) removal by BSH and FSH at pH = 6.0, initial Ni(II) conc. = 100 mg/L, contact time = 3 h, temp. = 25 ± 1 ℃, stirring speed = 180 rpm.

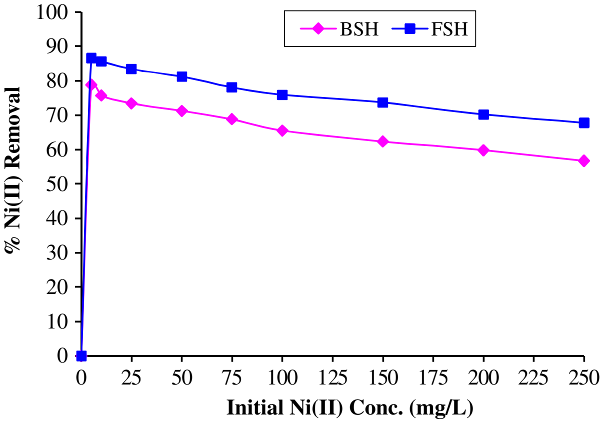

Fig. 6. Effect of initial concentration on Ni(II) removal by BSH and FSH at pH = 6.0, adsorbent dose = 20.0 g/L, contact time = 3 h, temp. = 25 ± 1 ℃, stirring speed = 180 rpm.

In case of BSH, the percent removal was lesser due to loss of some functional groups present on the adsorbent [21]. The unit adsorption increased with increase in initial Ni(II) concentration. It increased from 0.20 to 9.7 mg/g by BSH and 0.22 to 8.5 mg/g by FSH, respectively. This may be due to the fact that initial Ni(II) concentration contributes in the driving force to overcome mass transfer resistances of ions between the sorbent and bulk fluid phase. Higher initial concentrations enhance the mass transfer driving force, thus increasing the uptake [22].

### 3.5. Effect of contact time

To study the effect of contact time, Ni(II) solution (100 mg/L) was agitated in an orbital shaker at 180 rpm for different time intervals from 10 to 180 min at constant adsorbent dose (20.0 g/L) and temperature (25 ± 1 ℃). In the present study, this equilibrium was achieved within 120 min after which it became constant and there was no further Ni(II) adsorption. Hence, 180-min contact time was chosen as optimum time for further experiments so that complete equilibrium is achieved within this time period. The process was found to be very rapid initially, and a large fraction of the Ni(II) ions were removed within few minutes. This may be due to the fact that, during the initial stages of the process, a large number of vacant sites are available for adsorption. After some time, the remaining vacant sites are not easily available due to repulsive forces between the Ni(II) ions on the solid surface and the bulk phase. This results in slowing down of adsorption process during later period [18].

### 3.6. Effect of temperature

The experiments for Ni(II) adsorption were conducted in the temperature range of 15–55˚C at constant initial Ni(II) concentration (100 mg/L), pH (6.0), adsorbent dose (20.0 g/L) and contact time (180 min). It is evident from the results that Ni(II) adsorption increased with increase in temperature. Ni(II) adsorption increased from 56.2–80.1% by BSH and 63.7–92.7% by FSH with the increase in temperature indicating that the process is endothermic nature. The unit adsorption also increased with temperature. It increased from 2.8 to 4.0 from 15 to 55˚C by BSH and from 3.2 to 4.6 by FSH, respectively. The increase in unit adsorption with temperature may be attributed to enlargement of pore size or activation of adsorbent surface [23].

### 3.7. Equilibrium modeling and kinetic studies

Adsorption isotherms give the relationship between adsorbate concentration in the bulk and amount of adsorbent adsorbed at the interface and also gives certain constants by which the affinity of the adsorbent and its surface properties can be predicted.

The Langmuir equation applied to the experimental data is given in Eq. (3):

$$\frac{C_e}{q_e} = \frac{1}{Q_0 b} + \frac{C_e}{Q_0} \tag{3}$$

where $C_e$ and $q_e$ are same as in Eq. (2), $b$ determines the direction to which the equilibrium adsorbent (solid phase) + Ni (II) (aqueous phase) = adsorbent–Ni(II) moves. Higher values of $b$ indicate that the equilibrium moves to the right side resulting in the formation of the adsorbate–adsorbent complex and $Q_0$ is the maximum monolayer capacity of the adsorbents (mg/g). The plots of $C_e$ vs. $C_e/q_e$ are linear for the studied adsorbents. The values of $Q_0$ and $b$ were calculated from the slope and intercept of the Langmuir plot of $C_e$ vs. $C_e/q_e$. The maximum adsorption capacity ($Q_0$) was 16.26 and 12.76 mg/g by BSH and FSH, respectively. The values of coefficient of correlation $R^2$ for Langmuir isotherm are 0.7166 and 0.9485 for BSH and FSH, respectively (Table 2).

Table 2
Adsorption isotherms and kinetic models for Ni(II) adsorption onto BSH and FSH

| Biosorbent | BSH | FSH |
|---|---|---|
| Adsorption isotherms | | |
| *Langmuir parameters* | | |
| $Q_0$ (mg/g) | 16.26 | 12.76 |
| $b$ (L/mg) | 0.0088 | 0.021 |
| $R^2$ | 0.7166 | 0.9485 |
| *Freundlich parameters* | | |
| $K_f$ (mg/g) | 0.195 | 0.33 |
| $n$ (L/mg) | 1.237 | 1.314 |
| $R^2$ | 0.9955 | 0.9968 |
| *Kinetic models* | | |
| *Pseudo-first order* | | |
| $q_e$ (exp) (mg/g) | 3.28 | 3.8 |
| $q_e$ (cal) (mg/g) | 3.07 | 1.51 |
| $k_1$ (min$^{-1}$) | 0.0269 | 0.0166 |
| $R^2$ | 0.6695 | 0.661 |
| *Pseudo-second order* | | |
| $q_e$ (exp) (mg/g) | 3.28 | 3.8 |
| $q_e$ (cal) (mg/g) | 3.53 | 3.98 |
| $k_2$ (g/mg/min) | 0.0227 | 0.0272 |
| $R^2$ | 0.9983 | 0.9988 |

The analysis of Langmuir equation was also made on the basis of dimensionless constant called Langmuir separation factor ($R_L$) which indicates the favorability of the adsorption. Values of $R_L$ were calculated for the studied adsorbents using Eq. (4):

$$R_L = \frac{1}{1 + bC_i} \tag{4}$$

where $b$ and $C_i$ have already been mentioned.

If, $R_L > 1$, unfavorable adsorption,
$R_L = 1$, linear adsorption,
$0 < R_L < 1$, favorable adsorption,
$R_L = 0$, irreversible adsorption.

For the present study, the $R_L$ values were between 0 and 1 (0.0936–0.958) indicating the favorable adsorption of Ni(II) onto the adsorbents.

The Freundlich equation used in this study is given below in Eq. (5):

$$\log_{10} q_e = \log_{10}(K_f) + \left(\frac{1}{n}\right) \log_{10}(C_e) \tag{5}$$

where $K_f$ is the Freundlich constant (relative adsorption capacity of the adsorbent related to the binding energy) and constant $n$, is the heterogeneity factor that represents the deviation from linearity of adsorption. The plots of $\log_{10} C_e$ vs. $\log_{10} q_e$ were linear for the studied adsorbents. $K_f$ and $n$ were calculated from the slope and intercept of the Freundlich plot of $\log_{10} C_e$ vs. $\log_{10} q_e$. The values of coefficient of correlation, $R^2$, for Freundlich isotherm are 0.9955 and 0.9968 for BSH and FSH, respectively (Table 2). The relative adsorption capacity [$K_f$ (mg/g)] was 0.195 and 0.33 mg/g by BSH and FSH respectively. The data show that $R^2$ value was higher for Freundlich model, thus, indicating the applicability of Freundlich model for Ni(II) adsorption.

The adsorption intensity of the adsorbent ($n$) calculated from the Freundlich model (Table 2) was greater than 1.0 suggesting that the adsorption of Ni(II) on the studied adsorbents was a favorable physical process. Similar results have been reported by other others [24–26] for different adsorbents.

Lagergren equation was applied first assuming pseudo-first-order kinetics where the number of metal ions outnumbers the adsorption sites on the adsorbent surface:

$$\log_{10}(q_e - q_t) = \log_{10} q_e - \frac{k_1}{2.303}t \tag{6}$$

where $q_e$ and $q_t$ (both in mg/g) are the amounts of Ni(II) adsorbed at equilibrium time and at any time "$t$" (min), respectively, and $k_1$ is the equilibrium rate constant of pseudo-first-order equation (min$^{-1}$). The values of $k_1$ and $q_e$ were determined from the slope and intercept of the plot of $\log_{10} (q_e - q_t)$ vs. time and values of $k_1$ and $q_e$ are given in Table 2. Low values of correlation coefficient and disagreement between $q_e$ experimental and $q_e$ calculated values indicated that adsorption of Ni(II) onto BSH and FSH is not an ideal pseudo-first-order reaction.

As the validity of the first-order kinetics was low, the second-order model was applied to the data as given below:

$$\frac{t}{q_t} = \frac{1}{k_2 q_e^2} + \frac{1}{q_e}t \tag{7}$$

where $q_e$ and $q_t$ are same as in Eq. (6), and $k_2$ is the equilibrium rate constant of pseudo-second-order model (g/mg/min). The rate constant of pseudo-second-order model obtained from the plot of $t/q_t$ vs. *time* and the equilibrium adsorption capacity $q_e$ were calculated from the slope and intercept of the plots $t/q_t$ vs. *time*. The calculated $q_e$ values are comparable with experimental $q_e$ values (Table 2) and the correlation coefficient ($R^2$) is nearly equal to unity. This suggests that the adsorption of Ni(II) from aqueous solution onto studied adsorbents follows pseudo-second-order model.

BSH and FSH were compared in terms of their adsorption capacity (mg/g) with other adsorbents for the removal of nickel from aqueous solution. The adsorption capacities are presented in Table 3 [28–35].

Table 3
Unit adsorption capacity (mg/g) of various adsorbents for Ni(II) removal

| Adsorbents | Adsorption capacity (mg/g) | Reference |
|---|---|---|
| *Saccharum Bengalense* plant | 4.09 | [28] |
| Mustard oil cake | 1.3 | [29] |
| Sugarcane bagasse | 2.2 | [30] |
| Orange peel | 9.8 | [31] |
| *Moringa oleifera* wood | 17.5 | [32] |
| Waste Pomace | 14.8 | [33] |
| Rice husk | 5.4 | [34] |
| Oxidized coir fibers | 4.3 | [35] |
| BSH | 3.3 | Present study |
| FSH | 3.8 | Present study |

## 4. Desorption and regeneration studies

Desorption of any heavy metal from the exhausted adsorbent is necessary for the reuse of the adsorbents and recovery of metal ions. In the present study, an attempt was made to desorb Ni(II) from BSH and FSH using hydrochloric acid of different concentration (0.0125–0.20 M) for a contact period of 60 min.

The results showed that desorption was higher at higher HCl concentrations. However, optimum desorption was achieved at 0.125 M HCl. Desorption efficiency (%) increased with increase in HCl concentration (M). It increased from 57.2 to 88.7% in case of BSH as HCl concentration was increased from 0.0125 to 0.125 M, while it increased from 43.2 to 68.7% in case of FSH. Desorption became constant after 0.125 M after which there was no more desorption of Ni(II) ions from both the adsorbents. The higher desorption efficiency of Ni(II) may be due to the reason that protons ($H^+$) released from HCl competes with Ni(II) ions and displaces them from the surface of adsorbents because of higher electronegativity of $H^+$ ions (2.2) as compared to Ni(II) ions (1.9) [27].

## 5. Conclusion

This study showed that BSH and FSH are effective adsorbent for the removal of Ni(II) from aqueous solution. The maximum Ni(II) removal was 65.5 and 75.9% by BSH and FSH at pH=6.0, adsorbent dose = 20.0 g/L, initial Ni(II) concentration = 100 mg/L. The maximum adsorption capacity was 16.26 and 12.76 mg/g, respectively, by BSH and FSH. Adsorbents characterization showed that hydroxyl, carboxyl, amine, and carbonyl were the principal functional groups present on the surface of adsorbents. Value of coefficient of correlation (0.9968) showed that Freundlich model was applicable to the data. Pseudo-second-order model gave a better interpretation of the adsorption process. Ion exchange was identified to be the dominant mechanism for adsorption of Ni(II) by BSH and FSH. BSH and FSH can be the promising adsorbents that can be used by small-scale industries using batch or stirred-tank flow reactors.

## Acknowledgement

One of the authors (Monika Jain) is thankful to Council of Scientific and Industrial Research (CSIR), Govt. of India, New Delhi, for granting SRF to conduct this study.

## References

[1] K.A. Krishnan, K.G. Sreejalekshmi, R.S. Baiju, Ni(II) adsorption onto biomass based activated carbon obtained from sugarcane bagasse pith, Bioresour. Technol. 102 (2011) 10239–10247.

[2] Y.C. Sharma, V. Srivastava, S.N. Upadhayay, C.H. Weng, Alumina naoparticles for removal of Ni(II) from aqueous solution, Ind. Eng. Chem. Res. 47 (2008) 8095–8100.

[3] K. Kadirvelu, K. Thamaraiselvi, C. Namasivayam, Adsorption of nickel(II) from aqueous solution onto activated carbon prepared from coir pith, Sep. Purif. Technol. 24 (2001) 497–505.

[4] I. Villaescusa, N. Fiol, M. Martinez, N. Miralles, J. Poch, Removal of copper and nickel ions from aqueous solution by grape stalks wastes, Water Res. 38 (2004) 992–1002.

[5] B. Volesky, Sorption and Biosorption, BV Sorbex, Inc., Montreal Canada, 2003, p. 316.

[6] V.C. Taty-Costodes, H. Fauduet, C. Porte, A. Delacroix, Removal of Cd(II) and Pb(II) ions from aqueous solutions by adsorption onto sawdust of *Pinus sylvestris*, J. Hazard. Mater. B105 (2003) 121–142.

[7] N.M. Salem, A.L. Awad, Biosorption of Ni(II) from electroplating wastewater by modified (*Eriobotyra japonica*) loquat bark, J. Saudi Chem. Socie. (in press).

[8] G. Sun, X. Xu, Sunflower stalks as adsorbents for colour removal from textile wastewater, Ind. Eng. Chem. Res. 36 (1997) 808–812.

[9] G. Sun, W. Shi, Sunflower stalks as adsorbents for the removal of ions from wastewater, Ind. Eng. Chem. Res. 37 (1998) 1324–1328.

[10] N. Thinakaran, P. Baskarlingam, M. Pulikesi, P. Paneerselvam, S. Sivanesan, Removal of acid violet 17 from aqueous solutions by adsorption onto activated carbon prepared from sunflower seed hull, J. Hazard. Mater. 151 (2008) 316–322.

[11] M. Jain, V.K. Garg, K. Kadirvelu, Chromium(VI) removal from aqueous system using *Helianthus annuus* (sunflower) stem waste, J. Hazard. Mater. 162 (2009) 365–372.

[12] A. Galichet, G.D. Sockalingam, A. Belarbi, M. Manfait, FT-IR spectroscopic analysis of *Saccharomyces cerevisiae* cell walls: Study of an anomalous strain exhibiting a pink coloured phenotype, FEMS Microbiol. Lett. 197 (2001) 179–186.

[13] M. Iqbal, A. Saeed, S.I. Zafar, FTIR spectrophotometery, kinetics and adsorption isotherms modeling, ion exchange and EDX analysis for understanding the mechanism of $Cd^{2+}$ and $Pb^{2+}$ removal by mango peel waste, J. Hazard. Mater. 164 (2009) 161–171.

[14] L.R. Radovic, C. Moreno-Castilla, J. Rivera-Utrilla, Carbon Materials as Adsorbents in Aqueous Solution, Marcel Dekker, New York, 2000.

[15] K. Periasamy, C. Namasivayam, Removal of Ni(II) from aqueous solution and nickel plating industry wastewater using an agricultural waste: Peanut hulls, Waste Manage. 15 (1995) 63–68.

[16] A. Kapoor, Removal of heavy metals using fungus *Apergillus niger*, Bioresour. Technol. 70 (1999) 95–104.

[17] N. Friis, P. Myers-Keith, Biosorption of uranium and lead by *streptomyces longwoodensis*, Biotechnol. Bioeng. 28 (1986) 21–28.

[18] V.C. Srivastava, I.D. Mall, I.M. Mishra, Characterization of mesoporous rice hush ash (RHA) and adsorption kinetics of metal ions from aqueous solution onto RHA, J. Hazard. Mater. B 134 (2006) 257–267.

[19] E.A. Oliveira, S.F. Montanher, A.D. Andrade, J.A. Nobrega, M.C. Rollemberg, Equilibrium studies for the sorption of chromium and nickel from aqueous solutions using raw rice bran, Process Biochem. 40 (2005) 3485–3490.

[20] S.S. Shukla, L.J. Yu, K.L. Dorris, A. Shukla, Removal of nickel from aqueous solutions by sawdust, J. Hazard. Mater. B 121 (2005) 243–246.

[21] G. Yan, T. Viraraghvan, Effect of pretreatment on the bioadsorption of heavy metals on *Mucor rouxii*, Water SA 26 (2000) 119–123.

[22] F.A.A. Al-Rub, M.H. El-Naas, F. Benyahia, I. Ashour, Biosorption of nickel on blank alginate beads, free and immobilized algal cells, Process Biochem. 39 (2004) 1767–1773.

[23] P.P. Vishwakarma, K.P. Yadav, V. Singh, Nickel(II) removal from aqueous solution by adsorption on flyash, Pertanika 12 (1989) 357–366.

[24] A. Bhatnagar, K. Minocha, Biosorption optimization of nickel removal from water using *Punica granatum* peel waste, Colloids Surf. B: Biointer. 76 (2010) 544–548.

[25] M.E. Argun, S. Dursun, C. Ozdemir, M. Karatas, Heavy metal adsorption by modified oak sawdust: Thermodynamics and kinetics, J. Hazard. Mater. 141 (2007) 77–85.

[26] Z. Chen, W. Ma, M. Han, Biosorption of nickel and copper onto treated alga (*Undaria pinnatifida*): Application of isotherm and kinetic models, J. Hazard. Mater. 155 (2008) 327–333.

[27] A. Ewecharoen, P. Thiravetyan, W. Nakbanpote, Comparison of nickel adsorption from electroplating rinse water by coir pith and modified coir pith, Chem. Eng. J. 13 (2008) 181–188.

[28] M.I. Din, M.L. Mirza, Biosorption potentials of a novel green biosorbent *Saccharum bengalense* containing cellulose as carbohydrate polymer for removal of Ni (II) ions from aqueous solutions, Int. J. Bio. Macromol. 54 (2013) 99–108.

[29] M.A. Khan, M. Ngabura, T.S.Y. Choong, H. Masood, L.A. Chuah, Biosorption and desorption of Nickel on oil cake: Batch and column studies, Biores. Technol. 103 (2012) 35–42.

[30] I. Aloma, M.A. Martin-Lara, I.L. Rodriguez, G. Blázquez, M. Calero, Removal of Níkel(II) ions from aqueous solutions by biosorption on sugarcane bagasse, J. Taiwan Inst. Chem. Eng. 43 (2012) 275–281.

[31] N. Feng, X. Guo, S. Liang, Y. Zhu, J. Liu, Biosorption of heavy metals from aqueous solutions by chemically modified orange peel, J. Hazard. Mater. 185 (2011) 49–54.

[32] M.H. Kalavathy, L.R. Miranda, Moringa oleifera–a solid phase extractant for the removal of copper, nickel and zinc from aqueous solutions, Chem. Eng. J. 158 (2010) 188–199.

[33] Y. Nuhoglu, E. Malkoc, Thermodynamic and kinetic studies for environmental friendly Ni(II) biosorption using waste pomace of olive oil factory, Biores. Technol. 100 (2009) 2375–2380.

[34] K.K. Krishnani, X. Meng, C. Christodoulatos, V.M. Boddu, Biosorption mechanism of nine different heavy metals onto biomatrix from rice husk, J. Hazard. Mater. 153 (2008) 1222–1234.

[35] S.R. Shukla, R.S. Pai, A.D. Shendarkar, Adsorption of Ni(II), Zn(II), Fe(II) on modified coir fibers, Sep. Purif. Technol. 47 (2006) 141–147.

[36] J. Goel, K. Kadirvelu, C. Rajagopal, V.K. Garg, Investigation of adsorption of lead, mercury and nickel from aqueous solutions onto carbon aerogel, J. Chem. Technol. Biotechnol. 80 (2005) 469–476.

[37] K. Kadirvelu, P. Senthilkumar, K. Thamaraiselvi, V. Subburam, Activated carbon prepared from biomass as adsorbent: Elimination of Ni(II) from aqueous solution, Biores. Technol. 81 (2002) 87–90.

[38] C.F. Brasquet, Z. Reddad, K. Kadirvelu, P.L. Cloirec, Modeling the adsorption of metal ions ($Cu^{2+}$, $Ni^{2+}$, $Cd^{2+}$) onto ACCs using surface complexation models, Appl. Surf. Sci. 196 (2002) 356–365.